Derivation of an Effective Height for Scintillometers: La Poza Experiment in Northwest Mexico

O. K. HARTOGENSIS

Department of Meteorology and Air Quality, Wageningen University, Wageningen, Netherlands

C. J. WATTS AND J.-C. RODRIGUEZ

Instituto del Medio Ambiente y el Desarollo Sustenable, IMADES, Hermosillo, Sonora, Mexico

H. A. R. DE BRUIN

Department of Meteorology and Air Quality, Wageningen University, Wageningen, Netherlands

(Manuscript received 8 April 2002, in final form 17 March 2003)

ABSTRACT

The large-aperture scintillometer (LAS) is by now a generally accepted device for routinely obtaining the area-averaged sensible heat flux, *H*, on a scale of up to 10 km. It is an optical instrument that consists of a transmitter and receiver. In practice, the LAS beam height often varies along the path due to a variety of reasons. This study will explain what effective height to use in such situations, when analyzing scintillometer data to derive *H*. Several aspects are covered: a slanted path over flat terrain, structured terrain, and varying path height due to the curvature of the earth's surface.

To test the derived effective height formulation the authors present LAS data taken in September and October 1996 at a rangeland site in Sonora, Mexico. In experiment 1, the LAS was set up over a slant path, ranging roughly between 10 and 45 m above the surface over a 3200-m path. In experiment 2, a horizontal LAS path was used at approximately 30 m over a pathlength of 1100 m. The resulting sensible heat fluxes were compared with eddy-covariance data and show satisfactory results for both the full and one of the approximate formulations of the effective height.

1. Introduction

A scintillometer receiver measures intensity fluctuations in the radiation emitted by the transmitter. These fluctuations are caused by refractive scattering of turbulent eddies along the propagation path. From these measurements—depending on the transmitter source used—the structure parameters of temperature, C_T^2, or humidity, C_q^2, can be determined. From these, together with an estimate of the roughness length and wind speed measurements at a single level, the sensible heat flux, *H*, and latent heat flux, L_vE, can be calculated using Monin–Obukhov similarity theory (MOST).

Much of the theoretical work on the scintillometer method was done in the 1970s; see for example, Andreas (1990) and the overview article by Hill (1997). During the last decade more emphasis has been put on the application of the method to determine area-averaged fluxes of heat and water vapor at a scale of 1–10 km on a routine basis; see, for instance, the special issue on scintillometry in *Boundary-Layer Meteorology* (De Bruin 2002).

The ability to directly determine surface fluxes at these large scales is especially attractive to modelers. They need area-averaged fluxes as input for, or verification of their model at scales similar to, or greater than a model grid cell. Hydrological studies, that require fluxes at catchment scale, and remote sensing techniques, that need fluxes at the scale of a satellite pixel, are fields that benefit from the scintillometer method.

Different types of scintillometers have been developed. The large-aperture scintillometer (LAS) that is used in this study is an optical instrument with which C_T^2 and consequently *H* can be determined. Over the last decade, a great number of applied LAS studies have been presented, proving the LAS applicability to routinely obtain estimates of *H* at low cost. De Bruin et al. (1995) and McAneney et al. (1995) tested the LAS over a homogeneous surface. Meijninger et al. (2002b) showed the LAS can also be used to obtain *H* over heterogeneous surfaces. Poggio et al. (2000) used a LAS

Corresponding author address: O. K. Hartogensis, Department of Meteorology and Air Quality, Wageningen University, Duivendaal 2, 6701 AP Wageningen, Netherlands.
E-mail: oscar.hartogensis@wur.nl

with two detectors to measure crosswind speed over complex terrain. Beyrich et al. (2002) described a long-term study in which a LAS is used to determine fluxes on an operational basis. Watts et al. (2000) used a LAS for ''ground truth'' verification for fluxes derived from Advanced Very High Resolution Radiometer (AVHRR) satellite images. Kohsiek et al. (2002) deployed an extra large aperture scintillometer (XLAS) to obtain fluxes over a path length of almost 10 km. Of interest to hydrometeorological applications in particular are the LAS studies over wet/irrigated areas by Green and Hayashi (1998), Meijninger and De Bruin (2000), and Hoedjes et al. (2002), and the publications on radio wave scintillometry. With the radio wave scintillometer, C_q^2, and consequently L_vE can be determined (Green et al. 2001; Meijninger et al. 2002a).

Scintillometer measurements are increasingly performed over heterogeneous and nonflat terrain. In catchment studies, for example, measurements are required in a certain region of interest, where one often encounters nonideal circumstances. In addition, for scintillometer setups over large distances, the instrument is often installed on hills, or high structures, such as buildings, which might not be available at both ends of the path or are of different height, resulting in a slanted scintillometer beam.

In all these situations, the scintillometer beam height varies along the path. This means that the scintillometer measurements represent not only a horizontal, but also a vertical average of C_T^2. The average height of transmitter and receiver, in that case, does not represent the height of the vertically averaged C_T^2, because C_T^2 does not vary linearly with height, and the scintillometer signal is weighted towards the middle of the path. This is an important issue since H derived from the LAS C_T^2 measurements is particularly sensitive to the height of the instrument, as will be discussed in appendix A and section 4a.

In this study we will explain what effective height to use when analyzing scintillometer data to derive H. Several aspects will be covered: slanted path over flat terrain, structured terrain, varying path height due to the curvature of the earth, and footprint effects in cases of irregular variations upstream of the path.

To test the derived effective height formulations, we present LAS data taken during a field experiment in September and October 1996 at a rangeland site called La Poza in the Sonoran desert in northwest Mexico. We experimented with a LAS setup in which the heights of the transmitter and receiver above the surface were significantly different (factor of 5). To test the performance of the LAS under a ''normal'' situation, that is, for a horizontal path, we also deployed a LAS setup over a path that was more or less parallel to the surface. The LAS-derived sensible heat flux was compared with eddy-covariance data for both experiments. We will refer to the slant-path experiment as experiment 1 and to the horizontal-path experiment as experiment 2.

2. Theory

a. Determining the sensible heat flux, H, with a large-aperture scintillometer

The theoretical description of the LAS was first given by Wang et al. (1978). They derived the following expression relating the variance of the logarithm of the intensity fluctuations of the measured light intensity, $\sigma_{\ln(I)}^2$, to the structure parameter of the refractive index, C_n^2:

$$\sigma_{\ln(I)}^2 = \int_0^1 C_n^2(u)W(u)\, du. \tag{1}$$

$W(u)$ can be seen as a weighting function describing the contribution from $C_n^2(u)$ at each point along the path to the total LAS signal, $\sigma_{\ln(I)}^2$. It is given as

$$W(u) = 16\pi^2K^2L \int_0^\infty k\phi_n(k) \sin^2\left[\frac{k^2Lu(1-u)}{2K}\right] \times \left[\frac{2J_1(x_1)2J_1(x_2)}{x_1x_2}\right]^2 dk, \tag{2}$$

where $u = x/L$ is the dimensionless coordinate along a propagation path of length L, $K = 2\pi/\lambda$ is the optical wavenumber, k the turbulent spatial wavenumber, $\phi_n(k)$ is the three-dimensional spectrum of the refractive index in the inertial range ($\phi_n(k) = 0.033k^{11/3}$), and $J_1(x_1)$ and $J_1(x_2)$ are Bessel functions of the first kind with $x_1 = kDu/2$ and $x_2 = [kD(1-u)]/2$, where D is the aperture diameter. $W(u)$ has a bell-shaped form resulting in a maximum weight towards the middle of the path and zero weight near the transmitter and receiver.

Substituting Eq. (2) into Eq. (1) and integrating numerically, Wang et al. (1978) obtained

$$\overline{C_n^2} = 1.12\sigma_{\ln(I)}^2D^{7/3}L^{-3}, \tag{3}$$

where the overbar represents a spatial average.

In a turbulent medium like the atmosphere, both temperature and humidity fluctuations affect refractive index fluctuations. Thus, C_n^2 can be expressed as a function of its related variables C_T^2 and C_q^2, the structure parameters of temperature and humidity, respectively. For the visible and infrared regions of the electromagnetic spectrum—in which our LAS operates—temperature fluctuations, that is, C_T^2, dominate the C_n^2 signal. Under the assumption that the correlation coefficient between temperature and humidity, R_{Tq}, is positive and close to 1, Wesely (1976) derived a direct relationship between C_n^2 and C_T^2 where the humidity contribution to C_n^2 is expressed in terms of the Bowen ratio, Bo:

$$C_T^2 = C_n^2\left(\frac{T^2}{-0.78\cdot 10^{-6}P}\right)^2\left(1+\frac{0.03}{\text{Bo}}\right)^{-2}, \tag{4}$$

where T is temperature (K) and P is air pressure (Pa). In this study we will consider only unstable daytime conditions, where the condition $R_{Tq} = +1$ is approximately

met. Furthermore, it can be seen that whenever Bo $>$ $\sim$0.6, the humidity correction is less than 10%. For larger Bowen ratios, this term can be safely neglected.

According to MOST, C_T^2 made dimensionless with the temperature scale θ_* is a universal function of the stability parameter $Z_{\rm LAS}/L_{\rm MO}$:

$$\frac{C_T^2 Z_{\rm LAS}^{2/3}}{\theta_*^2} = f_T\left(\frac{Z_{\rm LAS}}{L_{\rm MO}}\right), \tag{5}$$

where $Z_{\rm LAS}$ is the LAS height, and $L_{\rm MO}$ the Monin–Obukhov length. For unstable conditions, Wyngaard et al. (1971) proposed

$$f_T\left(\frac{Z_{\rm LAS}}{L_{\rm MO}}\right) = c_1\left(1 - c_2\frac{Z_{\rm LAS}}{L_{\rm MO}}\right)^{-2/3}, \tag{6}$$

with $c_1 = 4.9$ and $c_2 = 7$. We used an adjusted value for $c_2 (c_2 = 6.1)$ after Andreas (1989) to reflect a von Kármán constant, $\kappa_{\rm kar}$, of 0.4 rather then 0.35 used by Wyngaard et al. (1971). To calculate the sensible heat flux, H, defined as $H = -\rho C_p u_* \theta_*$, an additional expression is needed to solve for u_*, the friction velocity. Usually, a standard Businger–Dyer flux-profile relation is used (see, e.g., Panofsky and Dutton 1984):

$$u^* = \frac{\kappa_{\rm kar} U}{\ln\left(\dfrac{Z_{\rm cup}}{z_0}\right) - \psi_m\left(\dfrac{Z_{\rm cup}}{L_{\rm MO}}\right) + \psi_m\left(\dfrac{z_0}{L_{\rm MO}}\right)}, \tag{7}$$

where z_0 is the roughness length, U the wind speed at height $Z_{\rm cup}$, and ψ_m is the integrated stability function for momentum, which for unstable conditions is defined as $\psi_m(Z_{\rm cup}/L_{\rm mon}) = 2\ln[(1 + x)/2] + \ln[(1 + x^2)/2] - 2\arctan(x) + \pi/2$, with $x = [1 - 16(Z_{\rm cup}/L_{\rm MO})]^{1/4}$. Next, the set of Eqs. (5)–(7) can be solved iteratively using $L_{\rm MO} = Tu_*^2/\kappa_{\rm kar} g\theta_*$ to give θ_* and u_* from which H follows from its definition. Here g is the gravitational acceleration.

It can be shown that H becomes independent of $L_{\rm MO}$ for very unstable (or so-called local free convection) conditions (e.g., Andreas 1991),

$$H = \rho c_p b Z_{\rm LAS}\left(\frac{g}{T}\right)^{1/2} (C_T^2)^{3/4}, \tag{8}$$

where $b = 0.47$ for $\kappa_{\rm kar} = 0.4$ and the empirical constants of Eq. (6), $c_1 = 4.9$ and $c_2 = 6.1$.

Whenever measurements are taken over tall and dense roughness obstacles, such as houses or trees, a displacement distance, d, should be applied such that $Z_{\rm LAS}$ and $Z_{\rm cup}$ in Eqs. (5) and (7) are replaced by $(Z_{\rm LAS} - d)$ and $(Z_{\rm cup} - d)$, respectively (see, e.g., Panofsky and Dutton 1984).

b. Derivation of an effective scintillometer height

In appendix A, the sensitivity of H to the LAS height, $Z_{\rm LAS}$ is investigated. There we show that for free convection conditions a relative error in $Z_{\rm LAS}$ causes an equal relative error in H [see also Eq. (8)]; whereas for neutral conditions, the relative error in H due to $Z_{\rm LAS}$ is half the relative error in $Z_{\rm LAS}$. The fact that H is so sensitive to $Z_{\rm LAS}$ indicates the importance of determining $Z_{\rm LAS}$ as accurately as possible. This, in turn, shows the relevance of introducing an effective LAS height for situations where the height of the LAS beam is not constant over the path.

From Eq. (4) it can be seen that C_n^2 and C_T^2 relate linearly to each other. Thus, combining Eqs. (1), (3), and (4) yields the path-averaged structure parameter of temperature, $\overline{C_T^2}$:

$$\overline{C_T^2} = \int_0^1 C_T^2(u) G(u)\, du, \tag{9}$$

where $G(u) = W(u)/\int_0^1 W(u)du$ is the weighting function describing the contribution of $C_T^2(u)$ at each point along the normalized path, u, to the total LAS weighted $\overline{C_T^2}$.

When the scintillometer beam does not have a constant height along the path, the resulting LAS weighted $\overline{C_T^2}$ represents both a horizontal and a vertical average of $C_T^2(u)$. The range in $C_T^2(u)$ due to a varying beam height can be very large, as C_T^2 is a strong function of height [see Eq. (5)]. To calculate H, however, a single value of $Z_{\rm LAS}$ is needed that corresponds best to the $\overline{C_T^2}$ measurement. We will call this value of $Z_{\rm LAS}$ the *effective height*, $Z_{\rm eff}$. By definition, the full expression for the effective height, $Z_{\rm eff\_Full}$ follows from Eq. (5):

$$\overline{C_T^2} \equiv \theta_*^2 f_T\left(\frac{Z_{\rm eff\_Full}}{L_{\rm MO}}\right) Z_{\rm eff\_Full}^{-2/3}. \tag{10}$$

Equally, for $C_T^2(u)$ along the path

$$C_T^2(u) \equiv \theta_*^2 f_T\left[\frac{Z(u)}{L_{\rm MO}}\right] Z(u)^{-2/3} \tag{11}$$

applies. $Z(u)$ is the scintillometer beam height along the path.

Substituting Eq. (10) and (11) into Eq. (9) and assuming a constant flux layer, that is, $d\theta^*/dz$ and $dL_{\rm MO}/dz$ are zero yields

$$Z_{\rm eff\_Full}^{-2/3} f_T\left(\frac{Z_{\rm eff\_Full}}{L_{\rm MO}}\right) = \int_0^1 Z(u)^{-2/3} f_T\left[\frac{Z(u)}{L_{\rm MO}}\right] G(u)\, du. \tag{12}$$

$Z_{\rm eff\_Full}$ is solved iteratively in conjunction with θ_* and u_* from the iterative procedure described in section 2a. Appendix B shows that substituting Eq. (6) into Eq. (12) produces a quadratic relation with a simple solution for $Z_{\rm eff\_Full}$. Note that the effective height depends on stability, and a different $Z_{\rm eff\_Full}$ is obtained for every C_T^2 averaging period.

It is important to note that the underlying fundamental assumption of Eq. (12), that is, the presence of a constant flux layer, means that C_T^2 is in equilibrium with the surface. For homogeneous, flat surfaces this is generally

true. For heterogeneous and structured surfaces this assumption still holds as long as the measurements are taken at a level above the top of the internal boundary layers of the heterogeneous patches, where the individual path signatures merge due to turbulent mixing. This height is often referred to as the blending height. Meijninger et al. (2002b) present a detailed study of the use of scintillometers over heterogeneous surfaces in terms of blending height and footprint of the measurements. They conclude that, for scintillometer measurements below the blending height over moderate heterogeneous surfaces, the violation of the assumptions underlying Eq. (12) is small and reliable fluxes can still be obtained if one accounts for the spatial flux distribution in the source area.

When the variation in height along the path is relatively small, the effective height can be estimated with a single value (as opposed to solving $Z_{\text{eff\_Full}}$ with Eq. (12) for every flux-averaging interval) with three levels of approximation.

The first approximation considers Eq. (12) for either neutral or free convection conditions. In these stability limits $Z_{\text{eff\_Full}}$ becomes stability independent. For the free convection case, that is, $Z_{\text{LAS}}/L_{\text{MO}} \rightarrow -\infty$, f_T as defined in Eq. (6) develops into $\lim_{Z_{\text{LAS}}/L_{\text{MO}} \rightarrow -\infty} f_T \propto Z_{\text{LAS}}^{2/3}$ as $|Z_{\text{LAS}}/L_{\text{MO}}| \gg 1$, and Eq. (12) simplifies to

$$Z_{\text{eff\_Fc}} = \left[\int_0^1 Z(u)^{-4/3} G(u)\, du\right]^{-3/4}. \tag{13}$$

For the neutral case, that is, $Z_{\text{LAS}}/L_{\text{MO}} \rightarrow 0$, f_T as defined in Eq. (6) develops into $\lim_{Z_{\text{LAS}}/L_{\text{MO}} \rightarrow 0} f_T \propto$ const, and Eq. (12) simplifies to

$$Z_{\text{eff\_Neutral}} = \left[\int_0^1 Z(u)^{-2/3} G(u)\, du\right]^{-3/2}. \tag{14}$$

The solutions for $Z_{\text{eff\_Full}}$ lie between $Z_{\text{eff\_Fc}}$ and $Z_{\text{eff\_Neutral}}$. Depending on the conditions, $Z_{\text{eff\_Full}}$ can be estimated by taking either $Z_{\text{eff\_Fc}}$ or $Z_{\text{eff\_Neutral}}$ or the average between the two.

The second approximation assumes that both the influences of stability and the $(-2/3)$ height-dependency of Eq. (12) are negligible, which results in

$$Z_{\text{eff\_WeightAvg}} = \int_0^1 Z(u) G(u)\, du, \tag{15}$$

where the subscript WeightAvg refers to the fact $Z(u)$ is weighted with weighting function $G(u)$. Meijninger and De Bruin (2000) used this approach.

The third approximation leaves scintillometer weighting function, $G(u)$, out of consideration—in addition to the assumptions made in Eq. (15)—and the arithmetic average of $Z(u)$, $Z_{\text{eff\_Avg}}$, remains

$$Z_{\text{eff\_Avg}} = \int_0^1 Z(u)\, du. \tag{16}$$

Note that in case hills are used to set up the scintillometer, the reduced surface elevation near the ends of the path will have a large effect on $Z_{\text{eff\_Avg}}$. It is then better to integrate $Z(u)$ between $0.15 < u < 0.85$, which, to a first order, simulates the effect of applying the weighting function $G(u)$.

It is difficult to quantify in a general way the error made when the proposed estimates are used instead of $Z_{\text{eff\_Full}}$. This is because the error depends on the variation of the beam height, the part of the path where the variation takes place, and, to a lesser extent, also on stability. These aspects will be different for each setup. Nonetheless, as a rule of thumb, the approximate estimates of $Z_{\text{eff\_Full}}$ can be used with little error when the difference in height between the highest and lowest point along the path between $0.15 < u < 0.85$ is less than a factor of 2. For most LAS setups, this criterion will be met.

In general, we can distinguish three conditions that cause $Z(u)$ to vary.

1) slant paths—the heights of transmitter and receiver are not equal;
2) topography—the surface under the scintillometer beam is not flat;
3) curvature of the earth's surface.

1) SLANT PATHS

To get an idea of how much $Z_{\text{eff\_Full}}$ differs from the arithmetically averaged beam height, $Z_{\text{eff\_Avg}}$, we consider a setup in which the scintillometer beam describes a slant path over a flat surface. With slant scintillometer paths, the beam height along the path, $Z(u)$, can be described in terms of Z_{high} and Z_{low}, respectively, the higher and lower heights of either transmitter or receiver:

$$\frac{Z(u)}{Z_{\text{low}}} = 1 + \left(\frac{Z_{\text{high}}}{Z_{\text{low}}} - 1\right)u. \tag{17}$$

On substituting Eq. (17) into Eqs. (13), (14), and (15), we can calculate $Z_{\text{eff\_Fc}}$, $Z_{\text{eff\_Neutral}}$, and $Z_{\text{eff\_Avg}}$ relative to Z_{low} as a function of $Z_{\text{high}}/Z_{\text{low}}$. These relations are depicted in Fig. 1a. A trivial result seen in Fig. 1a is that the slope of $Z_{\text{eff\_Avg}}/Z_{\text{low}}$ is 0.5. More noticeable, however, is that $Z_{\text{eff\_Netural}}/Z_{\text{low}}$ and $Z_{\text{eff\_Fc}}/Z_{\text{low}}$ show an almost perfect linear relation with $Z_{\text{high}}/Z_{\text{low}}$. With the regression lines specified in Fig. 1a, one can determine $Z_{\text{eff\_Fc}}$ and $Z_{\text{eff\_Neutral}}$ for slant paths based on the scintillometer setup, that is, Z_{high} and Z_{low}, with negligible error. The regression lines are determined for $Z_{\text{high}}/Z_{\text{low}} > 3$. Figure 1b shows the percentage error of using $Z_{\text{eff\_Avg}}$ rather then $Z_{\text{eff\_Fc}}$ or $Z_{\text{eff\_Neutral}}$ as a function of $Z_{\text{high}}/Z_{\text{low}}$.

2) TOPOGRAPHY

In practice, it is more common to encounter less variation in beam heights along the path than is shown in

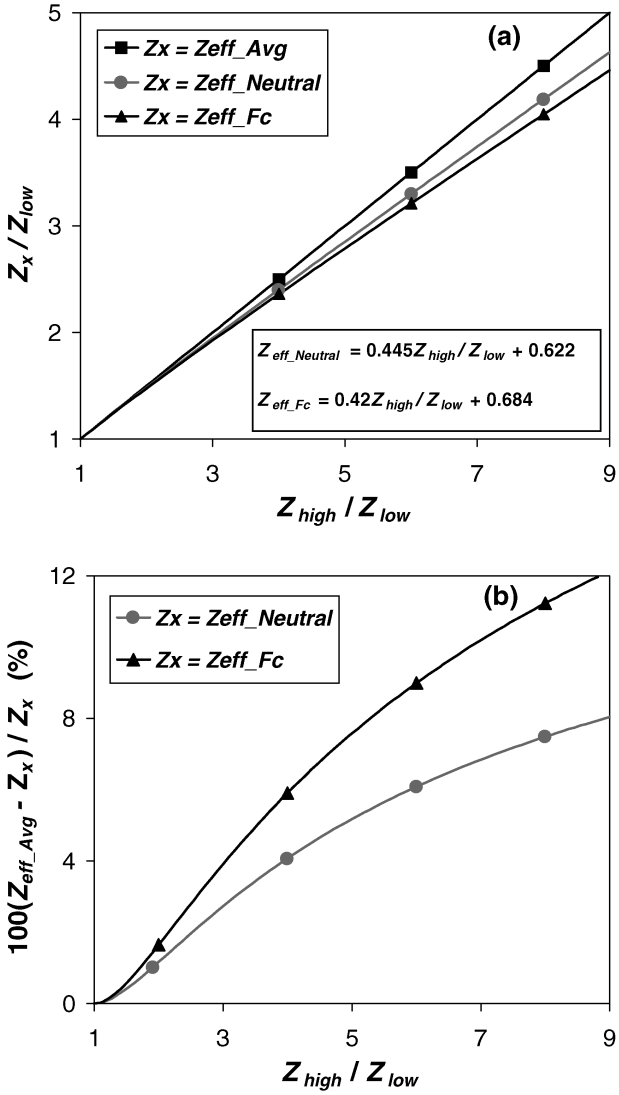

FIG. 1. Effective heights for neutral conditions, $Z_{\text{eff\_Neutral}}$, free convection conditions, $Z_{\text{eff\_Fc}}$, and the average height, $Z_{\text{eff\_Avg}}$, for a slant scintillometer beam path over a flat surface (a) as a function of the ratio of the high and low ends of the path, $Z_{\text{high}}/Z_{\text{low}}$. (b) Percentage error of using $Z_{\text{eff\_Avg}}$ rather then $Z_{\text{eff\_Neutral}}$ or $Z_{\text{eff\_Fc}}$ as a function of $Z_{\text{high}}/Z_{\text{low}}$.

Fig. 1. Typically, the height of transmitter and receiver are roughly the same, but topographic features cause the beam height to vary along the path. Height variations near the center of the path are particularly important because the weighting function has its maximum there. In contrast, the influence of the change in height and turbulence properties near both ends of the path, where the weighting function is zero, is negligible. This is a convenient circumstance, since hills or houses are often used to set up the scintillometer.

3) CURVATURE OF THE EARTH'S SURFACE

The curvature of the earth's surface affects the effective height whenever long scintillometer paths are used (Kohsiek et al. 2002). Correcting for the earth's curvature results in a pathlength-dependant reduction of the scintillometer beam height, $\Delta z_{\text{curve}}(u)$, along the path ranging from zero at $u = 0$ and $u = 1$, to a maximum at $u = 0.5$. Appendix C shows how $\Delta z_{\text{curve}}(u)$ is calculated. The correction in $Z_{\text{eff\_WeightAvg}}$ for the earth's curvature exceeds 0.5 m for pathlengths over 5 km.

Topography and the application of slant paths define the scintillometer height along the path relative to the surface. In case the earth's surface curvature correction, $\Delta z_{\text{curve}}(u)$ is important and a displacement distance is applicable, $Z(u)$ in Eqs. (11)–(16) should be taken as $[Z(u) - \Delta z_{\text{curve}}(u) - d]$.

In this paper we will only present data taken in the unstable stratified surface layer. For stable conditions, the effective height is, in principle, defined as in Eq. (12) with a stable MOST function for f_T. However, the constraint that there must a constant flux layer, which is generally true for the unstable case, may hold only to a certain degree for the weakly stable case. For stable to very stable conditions this condition will certainly not be met. Another issue is that the surface layer in the stable boundary layer (SBL) is often very shallow (only a few meters high), and scintillometers installed at great heights will be outside the region where MOST can be applied. On the other hand, in the SBL the sensitivity of H to Z_{LAS} is rather weak (Andreas 1989). Furthermore, although there are uncertainties in definition of Z_{eff} and the validity of MOST in the SBL, the absolute error in the flux due to these issues will generally be small, as the fluxes themselves are small. We recommend the use of $Z_{\text{eff\_WeightAvg}}$ of Eq. (15) in the SBL.

For other types of scintillometers, a similar derivation of the effective height applies. The difference is that the shape of the weighting function $G(u)$ depends on the type of scintillometer.

3. Site and instrument description

We conducted a field experiment in September and October 1996 at the La Poza rangeland site (~28.5°N, 110°W; ~200 m above sea level) 30 km south of Hermosillo, capital of the state of Sonora in northwest Mexico. The La Poza rangeland is used for extensive cattle farming. Nearly all the vegetation is natural and a vegetation survey showed that 25% of the area is covered with trees and bushes and the remaining 75% is short grass or bare soil. Bushes, trees, and cacti are generally not very tall, roughly ranging from 0.5 m to 5 m.

A MK2 Hydra one-dimensional eddy-covariance system (Institute of Hydrology, Wallingford, United Kingdom) was installed at 13.6 m on top of an 11-m-tall measurement tower. The Hydra consists of a fast-response cup anemometer (Vector Instruments, Rhyl, United Kingdom), a one-dimensional sonic anemometer, an infrared hygrometer, a thermocouple (all built at the Institute of Hydrology), and a REBS Q6 net radiometer

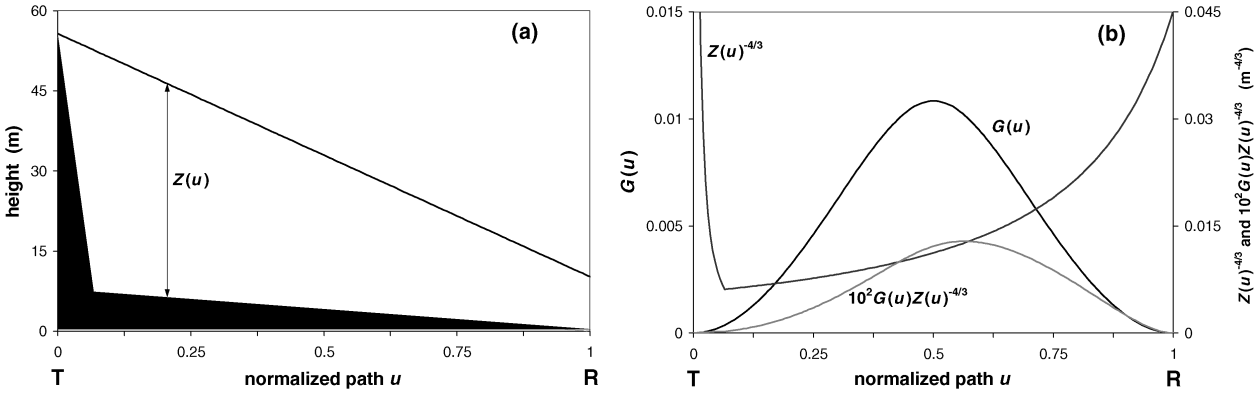

FIG. 2. Experiment 1: (a) Scintillometer beam height, $Z(u)$, along the normalized path, u. (b) Scintillometer weighting function, $G(u)$, height scaling of C_T^2 for free convection conditions, $Z(u)^{4/3}$, and the convolution between the two, $G(u)Z(u)^{4/3}$, which integrated over the path gives $Z_{\text{eff\_Fc}}$. T and R stand for transmitter and receiver respectively.

(Radiation and Energy Balance Systems, Inc., Seattle, Washington). It was designed as a simple, modular eddy-covariance system that includes data storage and data processing software (Shuttleworth et al. 1988). The software calculates fluxes for a fixed averaging interval of 60 min. We found that the u^* measurements of the Hydra were not reliable, that is, we were not able to obtain a reliable z_0-estimate from u_* applying standard MOST scaling laws. This is probably due to differences in response time between the sonic and cup anemometer.

Several net radiation and soil sensors were installed on and around the tower. A REBS Q7 net radiometer was installed over grass and bare soil. The REBS Q6 of the Hydra system mainly ''saw'' trees and shrubs. Soil heat flux measurements were performed with six REBS HFT3 soil heat flux plates, which were buried at ~5 cm-depth under different vegetation types, with a thermocouple placed above to account for heat storage in the top 5 cm. All these sensors were measured on one datalogger at 0.2 Hz and 60-min averages were stored. We averaged the measurements of the different sensors, where the weights were chosen to conform to the results of the vegetation study.

The LAS used in this study was designed and built at the department of Meteorology and Air Quality of Wageningen University, the Netherlands. The electronics are according to Ochs and Wilson (1993). It has an aperture diameter of 0.15 m, and the light source is a light-emitting diode operating at a peak wavelength of 0.94 μm, which is placed at the focal point of a concave mirror. The receiver employs an identical mirror to focus the light on a photo diode detector.

Scintillations appear as intensity fluctuations in the received signal. The received signal is bandpass filtered between 0.03 and 400 Hz. Sixty-minute averages of C_n^2, sampled at 1 Hz, were recorded. With Bowen ratio, wind and temperature data from the Hydra, these were subsequently processed to give 60-min averages of H.

The La Poza experiment consisted of two stages. Experiment 1 took place between 18 September and 17 October 1996. In total, 23 days of good data were collected during this period. The LAS was set up over a 3200-m path with the transmitter on top of a 50-m hill and the receiver on top of the eddy-covariance tower at a height of 12 m. Experiment 2 took place between 17 and 24 October 1996. The LAS was set up over an 1100-m path with the transmitter and receiver on top of two opposite hills, both at roughly 30 m above the surface.

The La Poza site is reasonably flat along the scintillometer paths and near the tower. Watercourses can be found at 500-m to 1-km intervals, in the vicinity of which the vegetation is relatively dense and high. Between the watercourses, there are more open patches with grass and bare soil. We can assume that this small-scale heterogeneity is blended below the LAS beam height for both setups, at least for the part of the path were the LAS weighting function is nonzero. The Hydra was set up at the transition of a more dense and a more open patch, such that its measurements can be considered representative of the LAS footprints.

Since we were not able to derive a reliable z_0-estimate from the Hydra, z_0 and d were determined from the vegetation survey. We estimated $z_0 = 0.15$ m and $d = 1.3$ m. A constant value for pressure of 990 hPa was used.

4. Results and discussion

a. Calculation of the effective height

Figure 2a illustrates the LAS beam along the path, $Z(u)$, for experiment 1. The height of the LAS beam and the elevation of the surface are given relative to the lowest point of the surface along the path. The surface elevation along the path is determined from a topographic map.

Figure 2b shows the different terms involved in calculating $Z_{\text{eff\_Fc}}$. It can be seen that the convolution between $G(u)$ and $Z(u)^{4/3}$ is skewed significantly towards the receiver part of the path, where the LAS beam is

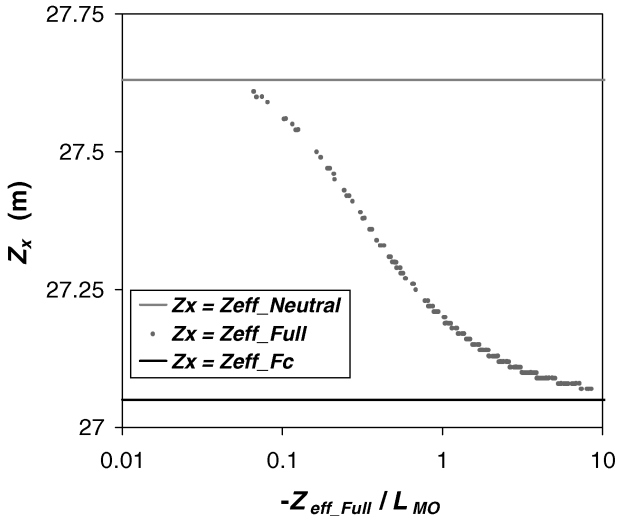

FIG. 3. Experiment 1: Iteratively determined effective height, $Z_{\text{eff\_Full}}$ from measurements using Eq. (12) as a function of stability, z/L_{MO}. Here, $Z_{\text{eff\_Neutral}}$ and $Z_{\text{eff\_Fc}}$ represent the neutral and free convection solutions of the effective height, respectively.

lowest. In other words, $Z_{\text{eff\_Fc}}$ is weighted toward the lower end of the scintillometer beam. It can also be seen that the influence of the hill, which gives considerable weight to $Z(u)^{4/3}$ near the transmitter end of the path, is negligible in $G(u)Z(u)^{4/3}$ because $G(u)$ tapers off to zero near both ends of the path.

The values of $Z_{\text{eff\_Neutral}}$, $Z_{\text{eff\_Fc}}$, and $Z_{\text{eff\_WeightAvg}}$ are given in Table 1, as well as some more conventional estimates of Z_{LAS} in these situations, $Z_{\text{eff\_Avg}}$ for $0.15 < u < 0.85$ and Z_{LAS} at midpoint, $u = 0.5$. It can be seen that the difference in height between $Z_{\text{eff\_Fc}}$ and $Z_{\text{eff\_Neutral}}$ is ~2%, and between $Z_{\text{eff\_Fc}}$ and the conventional estimates is ~7%. Figure 3 shows how the iteratively determined $Z_{\text{eff\_Full}}$ relates to $Z_{\text{eff\_Neutral}}$ and $Z_{\text{eff\_Fc}}$ as a function of stability.

Figure 4 depicts in a similar way as Fig. 2 how $Z_{\text{eff\_Fc}}$ is determined for experiment 2. Figure 4b shows that $G(u)Z(u)^{4/3}$ is hardly skewed to the lower end of the path because $Z(u)^{4/3}$ is almost constant over the part of

TABLE 1. For experiments 1 and 2: the effective heights calculated for free convection conditions, $Z_{\text{eff\_Fc}}$ from Eq. (13), neutral conditions, $Z_{\text{eff\_Neutral}}$ from Eq. (14), and weighted with LAS weighting function, $Z_{\text{eff\_WeightAvg}}$ from Eq. (15), and the more conventional height estimates, the average height between $0.15 < u < 0.85$, $Z_{\text{eff\_Avg}}$ after Eq. (16), and Z_{LAS} at midpoint, $u = 0.5$.

	$Z_{\text{eff\_Fc}}$ (m)	$Z_{\text{eff\_Neutral}}$ (m)	$Z_{\text{eff\_WeightAvg}}$ (m)	$Z_{\text{eff\_Avg}}$ (m)	Z_{LAS} at midpoint (m)
Exp 1	27.0	27.6	29.0	29.0	29.0
Exp 2	34.5	34.4	34.6	34.1	35.0

the path, which is weighted most by $G(u)$ (for $0.15 < u < 0.85$). From this it follows that the values of $Z_{\text{eff\_Neutral}}$, $Z_{\text{eff\_Fc}}$, and $Z_{\text{eff\_WeightAvg}}$ presented in Table 1 are nearly the same.

The influence of the earth's curvature has been taken into account in the effective height calculations although it was negligibly small: 0.1 m for experiment 1 and 0.02 m for experiment 2.

In Figs. 2a and 4a the surface elevation is given in a rather schematic way; that is, not every feature of the surface along the LAS beam is specified. This is done because for each stage of the path, the specified $Z(u)$ should be representative for the entire area seen by the LAS at that point.

In cases where the LAS footprint exhibits large differences in elevation in all directions, a different approach should be used. Meijninger et al. (2002b) presented a 3D LAS footprint function, which results from the convolution of the LAS weighting function, $G(u)$, and a footprint model describing how far downwind the LAS sees as a function of pathlength, wind speed, wind direction, and stability. The effective height is then evaluated by weighting a 3D field of the LAS height above the surface with the 3D footprint function.

Likewise, for each of the roughness parameters, z_0 and d, one value has to be found that is representative for the LAS footprint. If large differences in the surface roughness are present over the footprint, one could weigh the roughness variables quadratically, after, for example, Chehbouni et al. (1999).

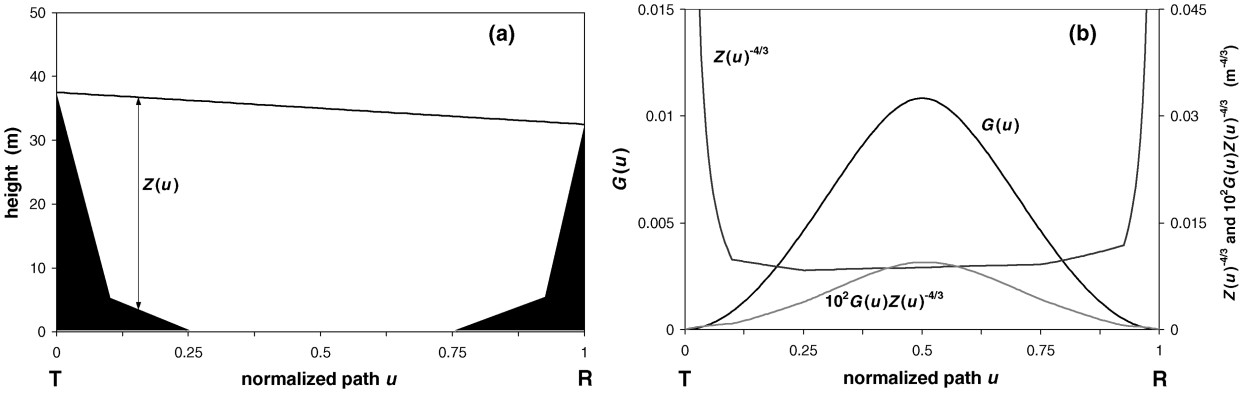

FIG. 4. Same as in Fig. 2 except for experiment 2.

Figure 1 gave us a sense of how much the effective height differs between applying $Z_{\text{eff\_Avg}}$, $Z_{\text{eff\_Fc}}$, and $Z_{\text{eff\_Neutral}}$ as a function of beam height variation along the path. Appendix A, then, illustrated the impact of these differences on H. To judge the full impact of the derived effective height, however, a sensitivity analysis would be needed that includes all input variables that go into the calculation of H. Andreas (1989) presents an extensive sensitivity study for a two-wavelength scintillometer method. It is beyond the scope of this paper to present such an analysis for the one wavelength LAS method. Instead, as an example, we will work out, for experiment 1 only, the relative contribution, dH_x_i, to the total relative error in H, dH, due to errors, δx_i, in the input variables, x_i, that go into the calculation of H. Here, dH is estimated as

$$dH = 100\left\langle \frac{\sqrt{\sum_{i=1}^{N}\{0.5[H(x_i + \delta x_i) - H(x_i - \delta x_i)]\}^2}}{H} \right\rangle,$$

where N is the number of input variables. Then, dH_x_i is

$$dH\_x_i = 100\left\langle \sqrt{\frac{\{0.5[H(x_i + \delta x_i) - H(x_i - \delta x_i)]\}^2}{(dH)^2}} \right\rangle.$$

The errors in the input variables were taken as follows: Z_{cup} (0.5 m), z_0 (0.05 m), T (1 K), Bo (50%), L (50 m), and P (20 hPa). We determined the error in Z_{LAS} by estimating the uncertainty in the surface elevation at each position along the path, which is mainly defined by its variation within the LAS footprint at that point. Weighted with Eq. (15), the total estimated error in Z_{LAS} results in 1.8 m, which includes an error estimate for d (0.2 m). This is ~7% of $Z_{\text{eff\_Full}}$. Coincidently, for experiment 1, the difference between the more conventional height estimates and $Z_{\text{eff\_Full}}$ is of the same order. The impact on H of the error in the estimation of Z_{LAS} and that of the use of simple Z_{LAS} estimates instead of $Z_{\text{eff\_Full}}$ will therefore be comparable.

In Table 2 a statistical summary is presented of dH_x_i, where $Z_{\text{eff\_Full}}$ from Eq. (12) has been used to calculate H. The total error in H, dH, is on the order of 10%. Clearly, the error in Z_{LAS} dominates dH. This also illustrates the impact of using simple estimates of Z_{LAS} instead of $Z_{\text{eff\_Full}}$. The second important contributor to dH is L. The strong power-3 dependence of C_n^2 to L is responsible for this [see Eq. (3)]. Especially for short pathlengths, where large relative errors in L are more likely to occur, it is very important to determine L as accurately as possible. The contributions to dH of errors in Z_{cup}, T, and P are negligible. Those of errors in z_0 and U are on the average small, but the high maximum values and standard deviations of the errors show they are important in some situations (neutral conditions). The contribution of Bo to dH is generally small as well, although it was assigned a 50% error. Only for very small Bo, $dH_$Bo is important. This due to the steep shape of the Bowen term in Eq. (4) for Bo < 0.6.

TABLE 2. Statistical summary of the percentage contribution, dH_x_i, to the total relative error in H, dH, due to errors, δx_i, in the input variables, x_i, that go into the calculation of H. The variables, x_i considered are: scintillometer height, Z_{LAS}, anemometer height, Z_{cup}, roughness length, z_0, temperature, T, pathlength, L, Bowen ratio, Bo, and Pressure, P.

		Range (%)		
	Mean (%)	Std dev	Min	Max
dH_Z_{LAS}	67	16	12	82
dH_Z_{cup}	0.03	0.07	0.00	0.34
dH_z_0	4	7	0	30
dH_U	6	11	0	48
dH_T	0.27	0.04	0.12	0.31
dH_L	14	2	6	16
$dH_$Bo	8	7	0	60
dH_P	0.70	0.27	0.05	1.18

Note that the impacts of possible violations of the theoretical assumptions behind Eqs. (1), (4), (5), and (12), have not been examined. Also, the impact of using another similarity function for f_T than Eq. (6) has not been included. Hill (1997) in his overview article summarizes the different functions found in the literature. It can be seen that for the neutral limit most functions agree quite well, whereas for the free convection limit differences can be found of up to 20% in H.

b. Comparison of LAS with eddy-covariance results

For experiment 1, Fig. 5 compares the 60-min averaged sensible heat fluxes from the LAS, H_{LAS}, and Hydra eddy-covariance system, H_{EC}. Only unstable conditions were analyzed, that is, data taken between 0800 and 1800 local time (LT). Figure 5a shows the comparison for H_{LAS} based on $Z_{\text{eff\_Full}}$ determined with Eq. (12). Figure 5b shows the comparison between H_{LAS} and H_{EC} for H_{LAS} based on $Z_{\text{eff\_WeightAvg}}$ determined with Eq. (15). In Table 3, the linear regression results for Fig. 5 are summarized.

It can be seen from Fig. 5 that H_{LAS} and H_{EC} compare reasonably, although a considerable scatter is observed. Using $Z_{\text{eff\_Full}}$ yields a marginally better fit than when the approximated $Z_{\text{eff\_WeightAvg}}$ is applied, that is, the rms of the fit is marginally better. On the other hand, the slope is closer to 1 for $Z_{\text{eff\_WeightAvg}}$. The differences between Figs. 5a and 5b are most apparent for large H, when the free convection limit is approached. This is because, under these conditions, the difference between the fixed $Z_{\text{eff\_WeightAvg}}$ and $Z_{\text{eff\_Full}}$ is largest (see Table 1 and Fig. 3), and H_{LAS} is most sensitive to Z_{LAS} (see appendix A).

Figure 5a will be used in the discussion of the results of H_{LAS} versus H_{EC} because it is based on a more accurately determined effective height. Two regions can

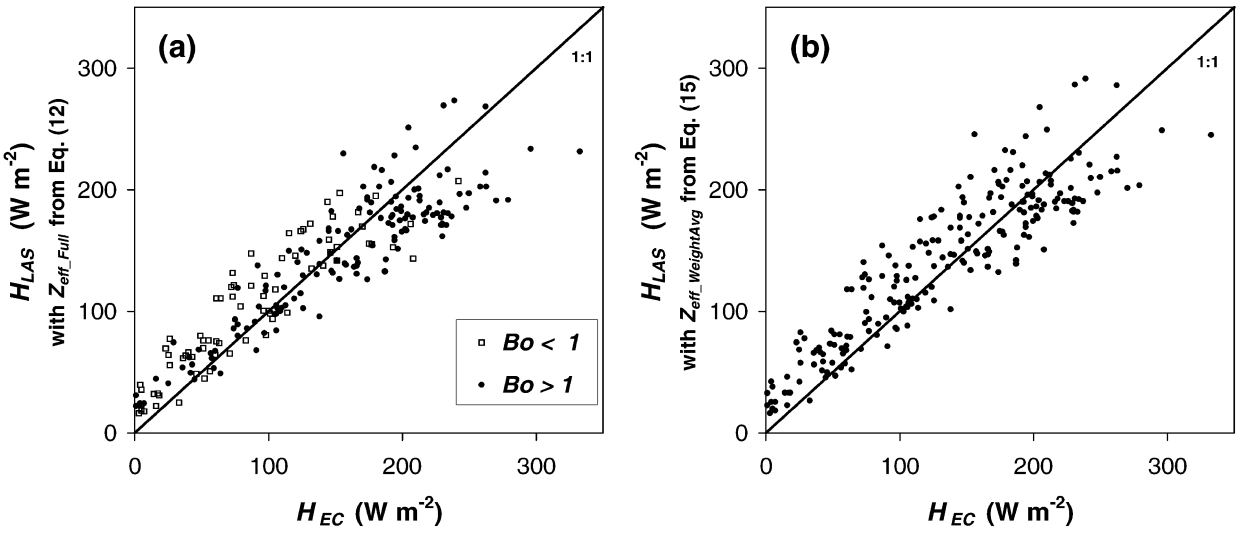

FIG. 5. Comparison for experiment 1 between 60-min averaged scintillometer and eddy-covariance sensible heat fluxes, H_{LAS} and H_{EC}, respectively. (a) H_{LAS} calculated with Z_{eff_Full} from Eq. (12). Different markers are used for Bowen ratio values, Bo, larger and smaller than 1. (b) H_{LAS} calculated with $Z_{eff\_WeightAvg}$ from Eq. (15).

be distinguished in Fig. 5a: one region in which the H_{LAS} overestimates H_{EC} (ranging roughly from 0 to 200 W m^{-2}), and another in which H_{LAS} underestimates H_{EC} (ranging from 150 W m^{-2} and higher). To discuss possible reasons behind these discrepancies between H_{LAS} and H_{EC}, we present Figs. 6 and 7.

Figure 6 shows H_{LAS} and H_{EC} as a function of the available energy for turbulent fluxes given by the net radiation, R_{net}, minus the soil heat flux, G. Only data points are shown for which both LAS and Hydra data were available. It can be seen that the Hydra produces more scatter than the LAS. We thus conclude that much of the scatter seen in Fig. 5 can be attributed to H_{EC}.

Figure 7 depicts the Bowen ratio, Bo, for experiment 1 and 2 (Fig. 7a) and the difference between H_{LAS} and H_{EC} relative to H_{EC} for experiment 1 (Fig. 7b) as a function of time. Only data between 0900 and 1600 LT are plotted to exclude fluxes near the morning and evening transitions when fluxes are small and the relative error in H and Bo can be very large. Prior to the experiment, a heavy thunderstorm brought 90 mm of rain, whereas during the experiment it did not rain at all. These conditions are reflected in the development of Bo during the experiment, which show that the experiments took place in drying conditions. The decrease in Bo around day of year (DOY) 280 is related to a frontal passage. We take Bo = 1 as the transition value between wet and dry conditions. Although there is a lot of scatter, a relation can be seen in Fig. 7 between Bo and the relative error between H_{LAS} and H_{EC}. In the beginning of the experiment, when the conditions were predominantly wet, H_{LAS} tends to overestimate H_{EC}, and, contrary, later in the experiment, when the conditions were predominantly dry, H_{LAS} tends to underestimate H_{EC}.

The *overestimation* of H_{LAS} seen in Fig. 5a corresponds for a large part with wet conditions, that is, nearly all points for Bo < 1 are above the 1:1 line. This is most likely due to absorption fluctuations of water vapor in the LAS signal caused by moisture-transporting eddies. Water vapor has strong absorption lines around 0.94 μm, the wavelength at which the

TABLE 3. Overview of linear regressions between the sensible heat fluxes of the scintillometer, H_{LAS}, and eddy covariance, H_{EC}. Regression parameters are specified for the zero-intercept model, $H_{LAS} = aH_{EC}$ and the nonzero-intercept model, $H_{LAS} = aH_{EC} + b$. The numbers in parentheses are uncertainties based on a 95% confidence interval.

		$H_{LAS} = aH_{EC}$			$H_{LAS} = aH_{EC} + b$			
	No. points	a (−)	r^2 (−)	rms (W m^{-2})	a (−)	b (W m^{-2})	r^2 (−)	rms (W m^{-2})
Exp 1 $Z_{eff\text{-}Full}$ from Eq. (12)	220	0.93 (0.013)	0.74	29.7	0.72 (0.022)	36.0 (3.4)	0.83	24.3
Exp 1 $Z_{eff\text{-}WeightAvg}$ from Eq. (15)	220	0.98 (0.014)	0.74	31.7	0.77 (0.024)	37.7 (3.7)	0.82	26.2
Exp 2 $Z_{eff\text{-}Full}$ from Eq. (12)	89	1.0 (0.017)	0.87	25.3	0.88 (0.032)	21.7 (5.2)	0.89	23.2

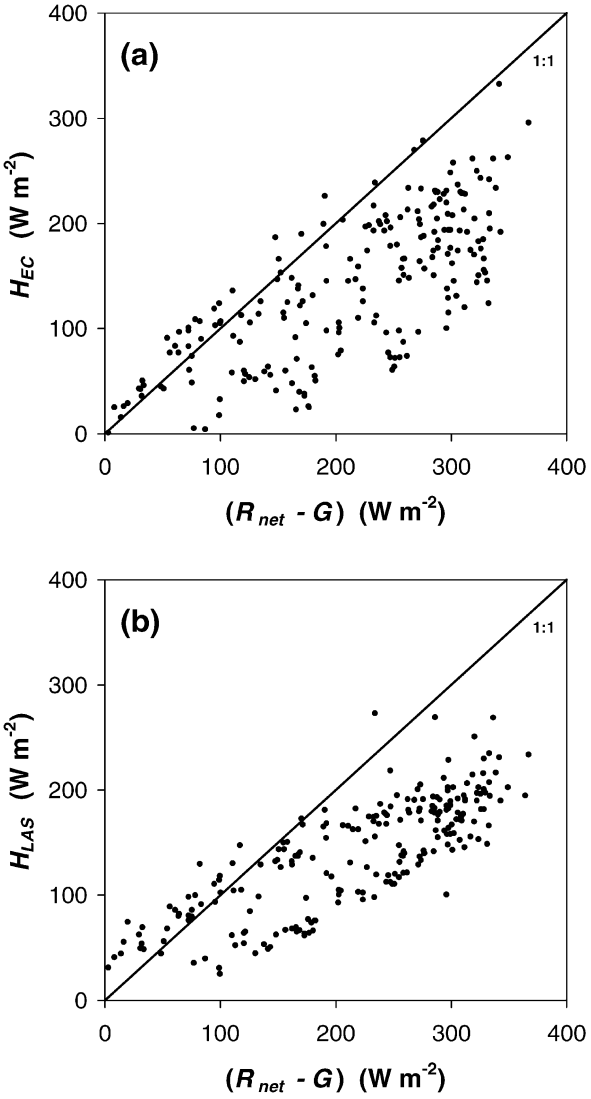

FIG. 6. Experiment 1: (a) Relation between the eddy-covariance heat flux, H_{EC}, and the net available energy for turbulent fluxes given by the difference in net radiation, R_{net}, and soil heat flux, G. (b) Same for scintillometer heat flux, H_{LAS}.

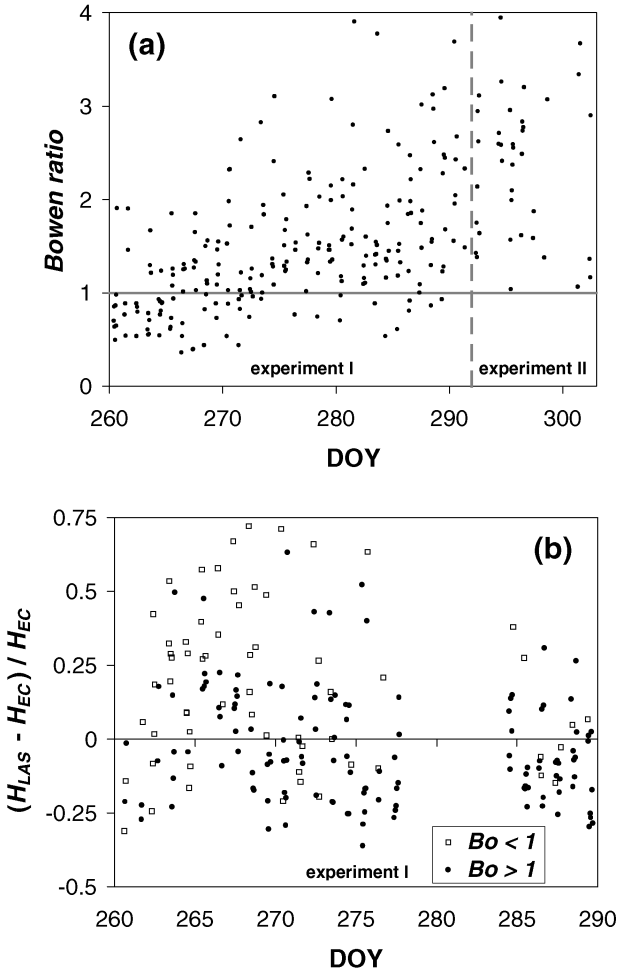

FIG. 7. (a) Bowen ratio as a function of day of year (DOY) for experiment 1 and 2, and (b) relative error between scintillometer heat flux, H_{LAS}, and eddy-covariance heat flux, H_{EC}, as a function of DOY for experiment 1. (b) Different markers are used for Bo larger and smaller than 1.

LAS operates. The LAS will erroneously interpret these absorption fluctuations as additional refractive index fluctuations, which finally results in a higher H_{LAS}. Scintillations due to absorption and refraction are spectrally separated at the low-frequency end of the spectrum. Using a similar LAS to that used in this study, Nieveen et al. (1998) found that the transition between the two regions lies between 0.071 and 0.36 Hz. The LAS we used in this study had a high-pass filter of 0.03 Hz and was therefore susceptible to absorption fluctuations. Based on the experiences with the La Poza experiment and the findings of Nieveen et al. (1998), the high-pass filter was changed to a cut off frequency of 0.1 Hz in later models.

One of the reviewers also pointed out that for near-neutral conditions, that is, small H, the LAS is under all circumstances sensitive to overestimation of H. Unlike, for instance, eddy-covariance instruments, the scintillometer cannot distinguish between ascending and descending warm air parcels (i.e., positive and negative H), and will record intensity fluctuations for both. Around neutral stability, ascending and descending warm air parcels are more likely to occur with the same intensity at the same time, and will thus result in a higher H_{LAS}. See, for example, Frederickson et al. (2000), who demonstrate that a bulk flux method, which is based on equations like Eqs. (5) and (6), underestimates C_n^2 near neutral stability.

The *underestimation* of H_{LAS} seen in Fig. 5a for high values of H, corresponds for the most part with dry conditions, that is, for $H > 150$ W m^{-2}, nearly all points below the 1:1 line are with Bo > 1. The cause of this

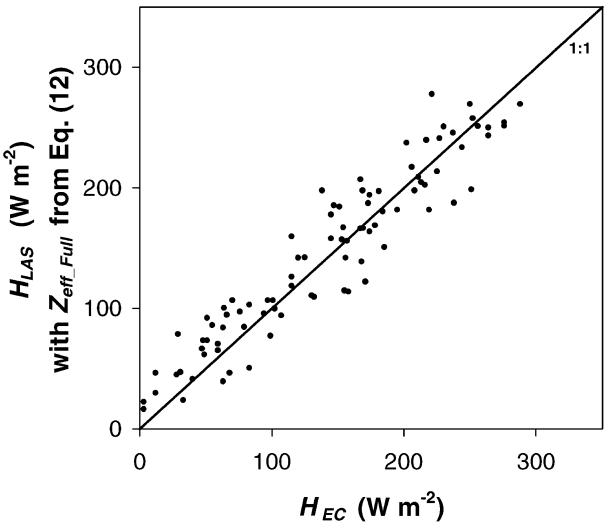

FIG. 8. Comparison for experiment 2 between 60-min averaged scintillometer and eddy-covariance sensible heat fluxes, H_{LAS} and H_{EC}, respectively.

is unclear. A hypothesis is that the LAS saturates, which means that measured intensity fluctuations above a certain level are no longer proportional to C_n^2. For the LAS, Ochs and Hill (1982) derived $C_n^2 < 0.185D^{5/3}\lambda^{1/3}L^{-8/3}$ as a saturation-free condition. Note that C_n^2 itself is a strong function of height [see Eq. (5)]. Since D and λ are instrument constants, z and L determine whether saturation occurs. In general, the longer the path, the higher the LAS needs to be installed to avoid saturation. For all points of Fig. 5a, the measured C_n^2 is within an order of magnitude of the saturation limit defined by Ochs and Hill (1982). For $H > 150$ W m^{-2}, this limit is approached to within 50%–80%. Saturation, therefore, possibly did occur for $H > 150$ W m^{-2} in the absence of the assumed effect of absorption fluctuations, that is, Bo > 1.

Figure 8 shows the comparison between the LAS and Hydra-derived sensible heat fluxes for experiment 2. The agreement between the two instruments and methods is better than in experiment 1 as can be seen from both Fig. 8 and Table 3. The hypotheses, which have been discussed earlier to explain the scatter that was observed in experiment 1 are less of an issue in experiment 2. To begin with, for unknown reasons less scatter was found for H_{EC} versus $(R_{\mathrm{net}} - G)$ than in experiment 1. Furthermore, absorption fluctuations were not expected to interfere with the LAS refractive index measurements during experiment 2, since the conditions were very dry. Neither was saturation of the LAS signal likely to be an issue with a shorter LAS pathlength, comparable LAS height, and similar atmospheric conditions to those at the end of experiment 1. The measured C_n^2 was two to three orders of magnitude below the saturation limit defined by Ochs and Hill (1982).

5. Conclusions

For many applications, the error in the scintillometer heat flux calculation, H, is for most part determined by the uncertainties in the estimated instrument height. These uncertainties arise in part from the error in estimating the height of the scintillometer along the path, and in part from the method by which one path integrated height value is obtained. In this paper, we focused on the latter issue. We derived an effective height for scintillometers as a function of stability, and discussed different sources of varying scintillometer beam height along the path. In addition, approximate formulations of the effective height have been proposed that are independent of stability.

In general, it can be concluded that to reduce the influence of a varying beam height on H, it is best to set up the transmitter and receiver as high as possible. First of all, if the instrument is above the so-called blending height, validity of similarity scaling is ensured, which is at the basis of the derived effective height and the flux calculations. Also, as is described in section 4a, the effect of small-scale topography along the path is blended. Secondly, slant paths are less likely to be an issue. The effective height for slant paths scales with ratio of the higher to the lower height of either transmitter or receiver. At high levels, an absolute difference in height between transmitter and receiver will affect this ratio to a lesser extent than at low levels. Finally, as one approaches the free convection limit at high levels, the stability dependence of the effective height vanishes and a single value can be used.

In most cases, however, the variation in height of the scintillometer beam along the path will not be very pronounced, and an approximate effective height formulation can be applied with little error. The influence of the earth's curvature exceeds 0.5 m for pathlengths over 5 km.

We experimentally tested the effective height formulation in terms of its effect on the heat flux. For the slant path experiment, we showed that using the stability-dependent effective height, a marginally better fit was found between LAS and eddy-covariance heat fluxes then with an approximated effective height, that is, the scatter was reduced. The horizontal path experiment yielded a better agreement between scintillometer and eddy-covariance fluxes. It is difficult to compare the results between these two experiments, as there were indications that for the slant path experiment the LAS heat fluxes were biased due to humidity absorption effects and possibly saturation of the scintillometer signal.

Acknowledgments. We thank Bert Heusinkveld for his assistance in installing the LAS, and Mike Stroud and John Stewart for their efforts in getting a Hydra system operational in La Poza. This study was financed by the European Union (CEC project C11 *CT91-0900).

APPENDIX A

H Sensitivity to Z_{LAS}

We will briefly discuss the sensitivity of the sensible heat flux, H, to the LAS height, Z_{LAS}, for unstable conditions to stress the importance of determining Z_{LAS} as accurately as possible and, thus, showing the relevance of the effective height proposed in this study.

When we combine the definitions of $H(H = -\rho C_p u_* \theta_*)$ and $L_{MO}(L_{MO} = Tu_*^2/\kappa_{kar} g\theta_*)$ with Eqs. (5) and (6), H can be written as

$$H = BZ_{LAS}\left(\frac{1 - c_2\dfrac{Z_{LAS}}{L_{MO}}}{-\dfrac{Z_{LAS}}{L_{MO}}}\right)^{1/2} \tag{A1}$$

with $B = \rho C_p\ (4.9)^{3/4}(C_T^2)^{3/4}(\kappa_{kar} g/T)^{1/2}$. The variables in B and the constant c_2 are specified in section 2a. The free convection expression of H given in Eq. (8) follows directly from Eq. (A1) for $Z_{LAS}/L_{MO} \to \infty$.

From Eq. (A1), we obtain the partial derivative of H with respect to Z_{LAS}:

$$\frac{\delta H/H}{\delta Z_{LAS}/Z_{LAS}} = \frac{1}{2}\left(\frac{1 - 2c_2\dfrac{Z_{LAS}}{L_{MO}}}{1 - c_2\dfrac{Z_{LAS}}{L_{MO}}}\right). \tag{A2}$$

Equation (A2) expresses the relative error in H due to a relative error in Z_{LAS} as a function of stability. Andreas (1989) derived a similar equation; see his Eq. (B22) and Fig. 3. Equation (A2) is plotted in Fig. A1, which shows that, for free convection conditions, a relative error in Z_{LAS} causes an equal relative error in H. For neutral conditions, on the other hand, the relative error in H due to Z_{LAS} is half the relative error in Z_{LAS}. This can also be seen directly from Eq. (A2).

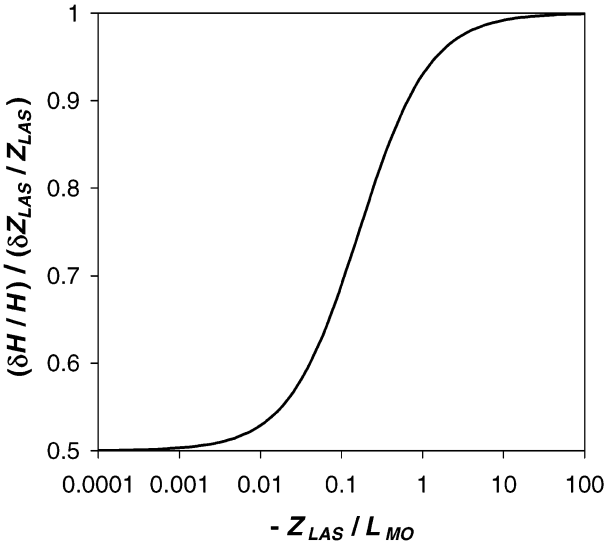

FIG. A1. The relative error in the sensible heat flux, H, due to a relative error in the scintillometer height, Z_{LAS}, as a function of stability, Z_{LAS}/L_{MO}.

APPENDIX B

Calculation of Z_{eff_Full} from Eqs. (6) and (12)

In this appendix, we derive an expression for Z_{eff_Full} from Eqs. (6) and (12). On substituting Eq. (6) into Eq. (12), one obtains, after rearranging the variables, the following quadratic equation for Z_{eff_Full}.

$$-\frac{c_2}{L_{MO}}Z_{eff\_Full}^2 + Z_{eff\_Full} - \left\langle \int_0^1 \left\{ Z(u)\left[1 - c_2\frac{Z(u)}{L_{MO}}\right]\right\}^{-2/3} G(u)\, du \right\rangle^{-3/2} = 0. \tag{B1}$$

Equation (B1) has only one solution for Z_{eff_Full} that is physically relevant:

$$Z_{eff\_Full} = \frac{-1 + \sqrt{1 - \dfrac{4c_2}{L_{MO}}\left\langle \displaystyle\int_0^1 \left\{ Z(u)\left[1 - c_2\frac{Z(u)}{L_{MO}}\right]\right\}^{-2/3} G(u)\, du \right\rangle^{-3/2}}}{\dfrac{-2c_2}{L_{MO}}}. \tag{B2}$$

From the set of Eqs. (5)–(7) and Eq. (B2), Z_{eff_Full}, θ_*, and u_* can now be iteratively solved using $L_{MO} = Tu_*^2/\kappa_{kar} g\theta_*$; H then follows from its definition, $H = -\rho C_p u_* \theta_*$.

APPENDIX C

Effect of the Earth's Curvature on the Effective Height

Figure C1 sketches how the earth's curvature affects (reduces) the height of the scintillometer along the propagation path. Here, Z_{LAS}, u, and $\Delta z_{\mathrm{curve}}(u)$ are as defined in section 2a. Normally, one assumes the scintillometer pathlength parallel to the earth's surface ($L_{//}$). In reality, however, the true pathlength, L, is straight, whereas the surface is slightly curved, which causes the scintillometer height to vary along the path. The difference in height between L and $L_{//}$ along the path is represented by $\Delta z_{\mathrm{curve}}(u)$, which should be evaluated as indicated in section 2b in obtaining an effective scintillometer height. Since $Z_{\mathrm{LAS}} \ll R_{\mathrm{earth}}$, the earth's radius ($R_{\mathrm{earth}} =$ 6387 km), $\Delta z_{\mathrm{curve}}(u)$ can be evaluated independently of Z_{LAS}:

$$\Delta z_{\mathrm{curve}}(u) = R_{\mathrm{earth}}\left\{1 - \frac{\cos(0.5\alpha)}{\cos[0.5\alpha - \beta(u)]}\right\}, \quad \text{(C1)}$$

with $\alpha = L/R_{\mathrm{earth}}$, and $\beta(u) = uL/R_{\mathrm{earth}}$.

Since the correction will always be small with respect to the overall scintillometer height, its effect along the path can be weighted according to Eq. (15) with negligible error. Figure C2 shows the total path weighted correction (reduction) for the earth's curvature as a function of pathlength. It can be seen that this correction exceeds 0.5 m for pathlengths over 5 km.

Note that the influence of the earth's curvature on the pathlength, L is negligible.

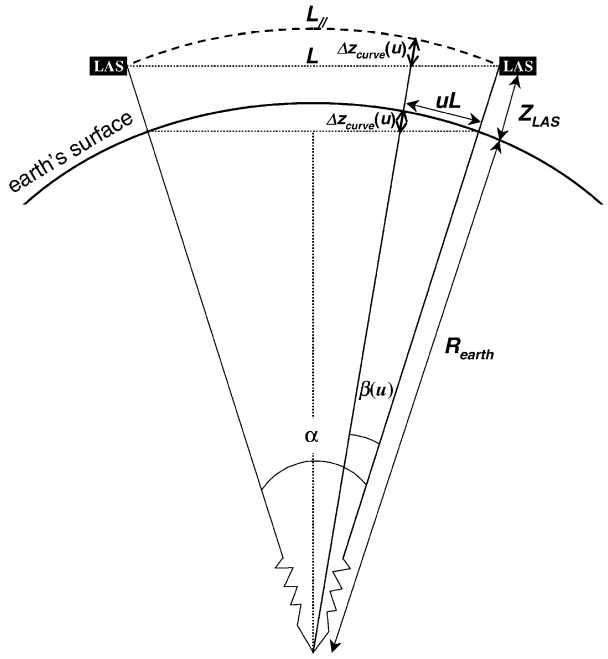

FIG. C1. Effect of the earth's curvature on the effective scintillometer height. The figure is not drawn to scale.

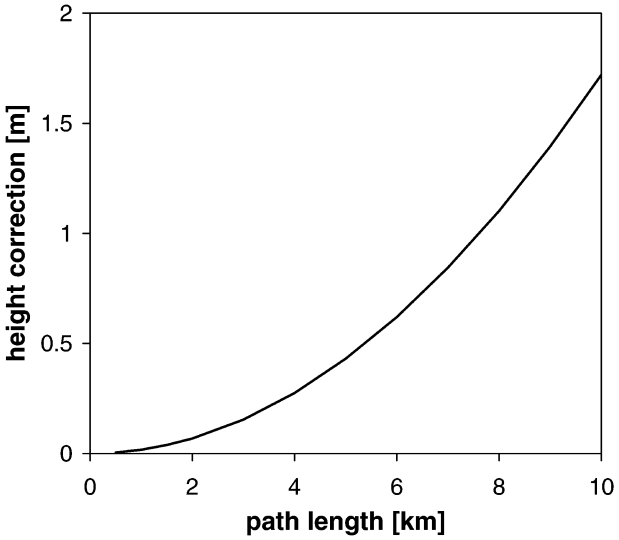

FIG. C2. The total path weighted correction (reduction), $\Delta z_{\mathrm{curve}}(u)$ for the earth's curvature as a function of pathlength.

REFERENCES

Andreas, E. L, 1989: Two-wavelength method of measuring path-averaged turbulent surface heat fluxes. *J. Atmos. Oceanic Technol.*, **6,** 280–292.

——, 1990: *Selected Papers on Turbulence in a Refractive Medium.* SPIE Milestone Series, Vol. 25, International Society for Optical Engineering, 693 pp.

——, 1991: Using scintillation at two wavelengths to measure path-averaged heat fluxes in free convection. *Bound.-Layer Meteor.*, **54,** 167–182.

Beyrich, F., H. A. R. De Bruin, W. M. L. Meijninger, and J. W. Schipper, 2002: Experiences from one-year continuous operation of a large aperture scintillometer over a heterogeneous land surface. *Bound.-Layer Meteor.*, **105,** 85–97.

Chehbouni, A., and Coauthors, 1999: Estimation of area-average sensible heat flux using a large-aperture scintillometer during the Semi-Arid Land-Surface-Atmosphere (SALSA) experiment. *Water Resour. Res.*, **35,** 2505–2511.

De Bruin, H. A. R., 2002: Introduction: Renaissance of scintillometry. *Bound.-Layer Meteor.*, **105,** 1–4.

——, B. J., J. M. Van den Hurk, and W. Kohsiek, 1995: The scintillation method tested over a dry vineyard area. *Bound.-Layer Meteor.*, **76,** 25–40.

Frederickson, P. A., K. L. Davidson, C. R. Zeisse, and C. S. Bendall, 2000: Estimating the refractive index structure parameter (C_n^2) over the ocean using bulk methods. *J. Appl. Meteor.*, **39,** 1770–1783.

Green, A. E., and Y. Hayashi, 1998: Use of the scintillometer technique over a rice paddy. *Japan. J. Agric. Meteor.*, **54,** 225–234.

——, M. S. Astill, K. J. McAneney, and J. P. Nieveen, 2001: Path-averaged surface fluxes determined from infrared and microwave scintillometers. *Agric. For. Meteor.*, **109,** 233–247.

Hill, R. J., 1997: Algorithms for obtaining atmospheric surface-layer fluxes from scintillation measurements. *J. Atmos. Oceanic Technol.*, **14,** 456–467.

Hoedjes, J. C. B., R. M. Zuurbier, and C. J. Watts, 2002: Large aperture scintillometer used over a homogeneous irrigated area, partly affected by regional advection. *Bound.-Layer Meteor.*, **105,** 99–117.

Kohsiek, W., W. M. L. Meijninger, A. F. Moene, B. G. Heusinkveld, O. K. Hartogensis, W. C. A. M. Hillen, and H. A. R. De Bruin, 2002: An extra large aperture scintillometer (XLAS) with a 9.8 km path length. *Bound.-Layer Meteor.*, **105,** 119–127.

McAneney, K. J., A. E. Green, and M. S. Astill, 1995: Large-aperture scintillometry: The homogeneous case. *Agric. For. Meteor.,* **76,** 149–162.

Meijninger, W. M. L., and H. A. R. De Bruin, 2000: The sensible heat fluxes over irrigated areas in western Turkey determined with a large aperture scintillometer. *J. Hydrol.,* **229,** 42–49.

——, A. E. Green, O. K. Hartogensis, W. Kohsiek, J. C. B. Hoedjes, R. M. Zuurbier, and H. A. R. De Bruin, 2002a: Determination of area-averaged water vapour fluxes with large aperture and radiowave scintillometers over a heterogeneous surface—Flevoland field experiment. *Bound.-Layer Meteor.,* **105,** 63–83.

——, O. K. Hartogensis, W. Kohsiek, J. C. B. Hoedjes, R. M. Zuurbier, and H. A. R. De Bruin, 2002b: Determination of area-averaged sensible heat fluxes with a large aperture scintillometer over a heterogeneous surface—Flevoland field experiment. *Bound.-Layer Meteor.,* **105,** 37–62.

Nieveen, J. P., A. E. Green, and W. Kohsiek, 1998: Using a large-aperture scintillometer to measure absorption and refractive index fluctuations. *Bound.-Layer Meteor.,* **87,** 101–116.

Ochs, G. R., and R. J. Hill, 1982: A study of factors influencing the calibration of optical C_n^2 meters. NOAA Tech. Memo. ERL WPL-106, NOAA/Environmental Research Laboratory, Boulder, CO, 24 pp.

——, and J. J. Wilson, 1993: A second-generation large-aperture scintillometer. NOAA Tech. Memo. ERL WPL-232, NOAA/Environmental Research Laboratory, Boulder, CO, 24 pp.

Panofsky, H. A., and J. A. Dutton, 1984: *Atmospheric Turbulence: Models and Methods for Engineering Applications.* John Wiley and Sons, 397 pp.

Poggio, P., M. Furger, A. S. H. Prévôt, W. K. Graber, and E. L Andreas, 2000: Scintillometer wind measurements over complex terrain. *J. Atmos. Oceanic Technol.,* **17,** 17–26.

Shuttleworth, W. J., J. H. C. Gash, C. R. Lloyd, D. D. McNeal, C. J. Moore, and J. S. Wallace, 1988: An integrated micrometeorological system for evaporation measurement. *Agric. For. Meteor.,* **43,** 295–317.

Wang, T. I., G. R. Ochs, and S. F. Clifford, 1978: A saturation resistant optical scintillometer to measure C_n^2. *J. Opt. Soc. Amer.,* **69,** 334–338.

Watts, C. J., A. Chehbouni, J. C. Rodríguez, Y. H. Kerr, O. Hartogensis, and H. A. R. De Bruin, 2000: Comparison of sensible heat-flux estimates using AVHRR with sctintillometer measurements over semi-arid grassland in northwest Mexico. *Agric. For. Meteor.,* **105,** 81–89.

Wesely, M. L., 1976: The combined effect of temperature and humidity on the refractive index. *J. Appl. Meteor.,* **15,** 43–49.

Wyngaard, J. C., Y. Izumi, and S. A. Collins Jr., 1971: Behavior of the refractive index structure parameter near the ground. *J. Opt. Soc. Amer.,* **15,** 1177–1188.